

NUMERICAL SIMULATION OF HALL THRUSTER PLASMA PLUMES

Iain D. Boyd

Department of Aerospace Engineering
University of Michigan, Ann Arbor, MI 48109, USA
Tel: (734) 615-3281; E-mail: iainboyd@umich.edu

Abstract

Hall thrusters are an important form of electric propulsion that are being developed and implemented to replace chemical systems for many on orbit propulsion tasks on communications and exploration spacecraft. A concern in the use of these devices is the possible damage their plasma plumes may cause to the host spacecraft. Computer models of Hall thruster plumes play an important role in integration of these devices onto spacecraft as the space environment is not easily reproduced in ground testing facilities. In this study, an advanced hybrid particle-fluid model is applied to model the plumes of the Hall thrusters used on the Russian Express and the European SMART-1 spacecraft. The results from the model are compared directly with measurements of ion current density and ion energy distributions taken in space by these spacecraft.

1. Introduction

Hall thrusters are under development in several countries including the United States, Russia, France, and Japan. These electric propulsion devices typically offer a specific impulse of about 1,600 sec and a thrust of about 80 mN. These characteristics make them ideally suited for spacecraft orbit maintenance tasks such as north-south station keeping. Under typical operating conditions, at a power level of about 1.5 kW, a voltage of 300 V is applied between an external cathode and an annular anode. The electrons emitted from the cathode ionize the xenon propellant efficiently aided by magnetic confinement within an annular acceleration channel (creating an azimuthal Hall current). The ions are accelerated in the imposed electric field to velocities on the order of 17 km/sec. New classes of Hall thrusters are being developed at low power (100 W) for use on micro-spacecraft, and at high power (25–100 kW) for spacecraft orbit-raising and planetary exploration.

As with any spacecraft propulsion device (chemical or electric), computer modeling is used to help assess any interactions between the plume of the thruster and the host spacecraft. In the case of Hall thrusters, there are three particular spacecraft integration issues: (1) the divergence angle of these devices is relatively large (about 60 deg) leading to the possibility of direct impingement of high energy propellant ions onto spacecraft surfaces that may result in sputtering and degradation of material properties. Material sputtered from spacecraft surfaces in this way may ultimately become deposited on other spacecraft surfaces such as solar cells, causing further problems; (2) back flow impingement of ions caused by formation of a charge exchange plasma; and (3) the high energy ions created inside the thruster cause significant erosion of the walls of the acceleration channel (usually made of metal or a ceramic such as boron nitride) and the erosion products may expand out from the thruster and become deposited on spacecraft surfaces.

A number of Hall thruster plume models have been developed.^{1–4} These models have been mainly assessed against detailed experimental data taken in the plumes of a variety of Hall thrusters in ground-based vacuum chambers. For a 1.5 kW class Hall thruster, the lowest background pressure that can be obtained in vacuum chambers is about 10^{-6} torr, which corresponds to an orbital altitude of about 185 km. Clearly, this represents a pressure that is orders of magnitude higher than that encountered in the operation of Hall thrusters in space. Another limitation of vacuum chambers concerns their size. Most Hall thruster plume measurements have been taken such that the maximum distance from the thruster that was probed was about 1 m.

The primary objective of this study is to assess a state-of-the-art Hall thruster plume model in terms of its predictions for realistic space conditions. The assessment is conducted through use of plasma plume measurements of Hall thrusters taken on board the Russian Express⁵ and the European SMART-1 spacecraft.⁶ The outline of the paper is as follows. First, an outline of the Express and SMART-1 spacecraft and their in-flight plume measurements is provided. Then, a description is given of the detailed hybrid particle-fluid plume model employed in this study. Results from the model are presented and comparisons made between measured and computed data for ion current density and ion energy distributions. The paper closes with some conclusions and suggestions for further work.

2. In-Flight Hall Thruster Plume Data

Both spacecraft considered here, Express and SMART-1, are currently in operation and employ xenon Hall thrusters with very similar operating conditions. A complete description of the two Russian Express-A GEO communications satellites and the flight data collection program are provided by Manzella et al.⁵ The thrusters employed are Russian SPT-100 models with a nominal thrust level of about 82 mN while operating at

a discharge current of 4.5 Amp and a total flow rate (anode plus cathode) of 5.3 mg/sec. A variety of sensors are employed on board the two spacecraft to characterize the effects of firing the Hall thrusters on the spacecraft operation and environment. These include electric field sensors, Faraday probes to measure ion current density, retarding potential analyzers (RPA's) to measure ion current and ion energy, and pressure sensors. In addition, disturbance torques on the spacecraft imparted by the Hall thruster plumes were recorded. From all of the above, the present study focuses on the RPA data for ion current density and ion energy distributions. The locations where RPA data is recorded are plotted in Fig. 1 with respect to an origin in the thruster exit plane on the thruster centerline. The variation in location is due to the firing of eight different thrusters and the fact that some of the sensors could be moved. Note that some of the sensors were as much as 8.8 m away from the thruster which is well in to the far-field region of the plume.

SMART-1 is a European mission to demonstrate solar electric propulsion by traveling to and then orbiting the Moon. A description of SMART-1, the Hall thrusters, and the plasma plume measurement instrumentation are provided by Tajmar et al.⁶ The thrusters employed are French PPS-1350 models that are largely based on Russian SPT-100 technology. The nominal thruster level is 70 mN with a current of 3.8 Amp and a flow rate of 4.2 mg/sec. These are similar enough to the conditions of the Express Hall thrusters that just one set of simulations is performed, at the Express thruster operating point.

3. Hall Thruster Plume Model

Hall thrusters primarily use xenon as propellant. The xenon plasma plume is composed of beam ions with velocities on the order of 16 km/s, low energy charge exchange ions, neutral atoms, and electrons. The total number density in the thruster is of the order of 10^{18} m^{-3} that places the plasma in the rarefied flow regime. Computational analysis of Hall thruster plumes is regularly performed using a hybrid particle-fluid formulation.¹ The direct simulation Monte Carlo (DSMC) method⁷ models the collisions of the heavy particles (ions and atoms). The Particle In Cell (PIC) method⁸ models the transport of the ions in electric fields. Overall, a hybrid approach is employed in which the electrons are modeled using a fluid description. In the present study, we employ a detailed treatment of the electron fluid by simultaneous solution of its three conservation equations.⁹

3.1 Plasma Dynamics

The most successful Hall thruster plume models are based on a hybrid approach in which heavy species are modeled using particles and the electrons modeled as a fluid. This is the approach adopted in the present study. Almost all previous hybrid models reduce the electron momentum equation to the Boltzmann relation:

$$\phi - \phi^* = \frac{kT_e}{e} \ln \left(\frac{n_e}{n^*} \right), \quad (1)$$

where n_e is the electron number density, * indicates a reference state, ϕ is the plasma potential, k is Boltzmann's constant, T_e is the constant electron temperature, and e is the electron charge. The potential is then differentiated spatially to obtain the electric fields. The Boltzmann relation requires that the electrons be collisionless, currentless, isothermal, and un-magnetized. All of these assumptions are questionable in a Hall thruster plume, particularly in the plume near-field. Despite the simplicity of the model, hybrid methods based on the Boltzmann relation have been quite successful in simulating the far-field properties of a number of different Hall thrusters.¹

In the present study, a detailed fluid electron model is employed that uses all three electron conservation equations. The model has been described in detail elsewhere and applied to the near field of a 200 W Hall thruster operated in a test chamber.⁹

The electron continuity equation is:¹⁰

$$\frac{\partial}{\partial t}(n_e) + \nabla \cdot (n_e \mathbf{v}_e) = n_e n_a C_i \quad (2)$$

where n_e is the electron number density, \mathbf{v}_e is the electron velocity vector, n_a is the atomic number density, and C_i is the ionization rate coefficient. Assuming steady flow, this equation is transformed into a Poisson equation by introducing a stream function ψ using

$$n_e \mathbf{v}_e = \nabla \psi \quad (3)$$

such that

$$\nabla^2 \psi = n_e n_a C_i, \quad (4)$$

for which numerical solutions are obtained using the standard Alternating Direction Implicit (ADI) method. The spatial distribution of the ion particles gives the electron number density, n_e , under the assumption of charge neutrality. This allows the electron velocity vector to be determined through solution of Eq. (4). In the present study, the xenon ionization rate coefficient is set to zero due to the low temperatures involved.

In the absence of magnetic field effects, the electron momentum equation is given by¹⁰

$$\frac{\partial}{\partial t}(m_e n_e \mathbf{v}_e) + m_e n_e (\mathbf{v}_e \cdot \nabla) \mathbf{v}_e = -en_e \mathbf{E} - \nabla p_e + \mathbf{R} \quad (5)$$

where m_e is the mass of an electron, \mathbf{E} is the electric field, p_e is the electron pressure, and \mathbf{R} is the friction term. It is further assumed that the electrons behave as a perfect gas ($p_e = n_e k T_e$), and that the friction term is given by

$$\mathbf{R} = \frac{en_e \mathbf{j}}{\sigma} \quad (6)$$

where \mathbf{j} is the current density, and σ is the electrical conductivity.

Assuming a steady state, neglecting the inertial term on the left hand side of Eq. (5), and introducing the plasma potential $-\nabla\phi = \mathbf{E}$, a generalized Ohm's law is obtained:

$$\mathbf{j} = \sigma \left[-\nabla\phi + \frac{1}{en_e} \nabla(n_e k T_e) \right] \quad (7)$$

For given n_e , \mathbf{v}_e , and T_e , the charge continuity condition:

$$\nabla \cdot \mathbf{j} = 0 \quad (8)$$

is then solved to obtain the plasma potential. This equation is written as a Laplace equation with weak source terms and is again solved using an Alternating Direction Implicit (ADI) scheme.

The electron energy equation is given by¹⁰

$$\frac{\partial}{\partial t} \left(\frac{3}{2} n_e k T_e \right) + \frac{3}{2} n_e (\mathbf{v}_e \cdot \nabla) k T_e + p_e \nabla \cdot \mathbf{v}_e = \nabla \cdot \kappa_e \nabla T_e + \mathbf{j} \cdot \mathbf{E} - 3 \frac{m_e}{m_i} \nu_e n_e k (T_e - T_H) - n_e n_a C_i \varepsilon_i \quad (9)$$

where m_i is the ion mass, ν_e is the total electron collision frequency, κ_e is the electron thermal conductivity, and T_H is the heavy particle temperature. Again assuming a steady state, and dividing by the thermal conductivity:

$$\nabla^2 T_e = -\nabla \ln(\kappa_e) \cdot \nabla T_e + \frac{1}{\kappa_e} \left(-\mathbf{j} \cdot \mathbf{E} + \frac{3}{2} n_e (\mathbf{v}_e \cdot \nabla) k T_e + (p_e \nabla \cdot \mathbf{v}_e + 3 \frac{m_e}{m_i} \nu_e n_e k (T_e - T_H) + n_e n_a C_i \varepsilon_i) \right) \quad (10)$$

where \mathbf{j} is obtained from Eq. (7) after the plasma potential is calculated. Equation (10) is again a Laplace equation with weak source terms that is solved using the ADI approach.

Finally, the electron transport coefficients are evaluated using their basic definitions:¹⁰

$$\sigma = \frac{e^2 n_e}{m_e \nu_e} \quad (11)$$

$$\kappa_e = \frac{2.4}{1 + \frac{\nu_{ei}}{\sqrt{2}\nu_e}} \frac{k^2 n_e T_e}{m_e \nu_e} \quad (12)$$

where $\nu_e = \nu_{ei} + \nu_{en}$, ν_{ei} is the ion-electron collision frequency, ν_{en} is the neutral-electron collision frequency, and these frequencies are evaluated for the xenon system using cross sections provided in Ref. 10. Note that, for each time step, the numerical scheme iterates several times through the solution of Eqs. (8) and (10) due to the coupling between ϕ and T_e .

3.2 Collision Dynamics

The DSMC method uses particles to simulate collision effects in rarefied gas flows by collecting groups of particles into cells which have sizes of the order of a mean free path. Pairs of these particles are then selected at random and a collision probability is evaluated that is proportional to the product of the relative velocity and collision cross section for each pair. The probability is compared with a random number to determine if that collision occurs. If so, some form of collision dynamics is performed to alter the properties of the colliding particles.

There are two basic classes of collisions that are important in the Hall thruster plumes: (1) elastic (momentum exchange); and (2) charge exchange. Elastic collisions involve only exchange of momentum between the participating particles. For the systems of interest here, this may involve atom-atom or atom-ion collisions. For

atom–atom collisions, the Variable Hard Sphere (VHS)⁷ collision model is employed. For xenon, the collision cross section is

$$\sigma_{EL}(\text{Xe}, \text{Xe}) = \frac{2.12 \times 10^{-18}}{g^{2\omega}} \text{m}^2, \quad (13)$$

where g is the relative velocity, and $\omega=0.12$ is related to the viscosity temperature exponent for xenon.

Both atom–ion momentum and charge exchange processes are modeled using the same cross section that was developed by Boyd and Dressler² based on a combination of theory and experiment:

$$\sigma_{CEX}(\text{Xe}, \text{Xe}^+) = (-13.6 \log_{10}(\varepsilon) + 87.3) \times 10^{-20} \text{m}^2. \quad (14)$$

where $\varepsilon = \frac{1}{2}m^*g^2$ and is measured in eV, and m^* is the reduced mass. Reference 2 also recommends that charge exchange cross sections for the interaction where a doubly charged ion captures two electrons from an atom are a factor of two lower than the values for the singly charged ions at corresponding energies. Charge-exchange collisions are simulated using the differential cross sections developed in Ref. 2. Momentum exchange collisions assume either the same differential scattering cross sections, or isotropic scattering.

3.3 Boundary Conditions

For the computations of Hall thruster plumes, boundary conditions must be specified at several locations: (1) at the thruster exit; (2) at the cathode exit; (3) along the outer edges of the computational domain; and (4) along all solid surfaces in the computational domain.

Several macroscopic properties of the plasma exiting the thruster are required for the computations. For the electrons, their current, temperature, and the plasma potential must be specified. For each of the heavy species (Xe , Xe^+ , Xe^{2+}) we require the number density, velocity, and temperature. In the real device, these properties vary radially across the exit plane. The approach to determining these properties involves a mixture of analysis and estimation. The basic performance parameters of mass flow rate, thrust, and total ion current are assumed to be known. The neutrals are assumed to exit the thruster at the sonic speed corresponding to some assumed value for their temperature. Finally, divergence angles for the lower and upper edges of the exit channel must be assumed. Combining all this information then allows all species densities and the velocities to be determined. Determination of the properties of multiple charge states, for example Xe^{2+} is considered in the present study, requires knowledge of the current fraction of that state.

In the electron fluid model, the external cathode of the Hall thruster must be modeled. While the actual cathode provides essentially a point source of electrons that therefore involves a three dimensional flow, in the present study it is modeled within the axially symmetric framework of the code. This is not a bad assumption given the high mobility of the electrons that rapidly form a symmetric flow field. The boundary conditions required for the electrons at the exit of the cathode are the electron current, the plasma potential, and the electron temperature.

Both fluid and particle boundary conditions are required at the outer edges of the computational domain. The electron fluid conditions employ either Dirichlet (fixed value) or Neumann (fixed gradient) boundary conditions. For the simulation of a spacecraft plume in space, these conditions are difficult to determine. In the present case, the gradients of electron current normal to the domain edges are set to zero, and the plasma potential on all domain boundaries is set to -5 V. The electron temperature along the upper edge of the domain is set to 0.2 eV, and zero gradient in electron temperature is set along the right-hand and left-hand domain edges. The heavy particle boundary condition is to simply remove from the computation any particle crossing any domain edge.

The solid wall surfaces of the Hall thruster are also included in the computation. Along these walls, a fixed value (1 eV) of the electron temperature is usually employed. The front face of the thruster is sprayed with di-electric material and so a condition of zero current is employed to calculate the plasma potential. In terms of heavy particles, any ions colliding with the walls are neutralized. Both atoms and neutralized ions are scattered back into the flow field from the surface of the thruster wall assuming diffuse reflection at a temperature of 500 K.

4. Results

As discussed above, the Hall thrusters employed on the Express and SMART-1 spacecraft are very similar, and so just one simulation condition is considered. As there are more data available from the Express spacecraft at this time, we employ the conditions for the SPT-100 Hall thruster.

At the thruster exit, the densities and temperatures are assumed to be radially uniform, the velocities are based on a divergence angle of 25 deg., an ion temperature of 1 eV is assumed, and the densities and velocities are obtained from the mass flow rate and integrated ion current. The thruster exit plasma flow conditions are listed in Table 1. The conditions at the cathode exit employ an electron current equal to the discharge current of 4.5 A, a plasma potential of 0 V, and an electron temperature of 1 eV.

The computational domain extends more than 10 m axially from the thruster exit and 10 m radially from the thruster centerline to cover all of the Express probe locations. This is achieved using a mesh containing 190 by 175 non-uniform, rectangular cells. In a typical computation approximately 4 million particles are employed with about 60% representing ions (both single and double charged). The neutral atom flow is first allowed to reach a steady state by using a large time step. The ions are then subsequently introduced with a time step of about 10^{-7} sec. The computations reach a steady state for the ions after about 15,000 iterations and solutions are then averaged over a further 10,000 iterations. The total computation time is about 24 hours on a personal computer.

Before making comparison with the flight data, we first consider some general properties of the plume simulation. In Fig. 2, contours of plasma potential are shown. The bubble like structure directly above the thruster exit (located at $Z=0$ m) is caused by the charge exchange collisions. It is this region that is of primary interest in spacecraft integration concerns due to the acceleration of ions into the back flow region. In Fig. 3, the contours of electron temperature are provided. Thermal conductivity is found to be the primary mechanism affecting the structure of this property.

In Figs. 4 and 5, contours are shown of the plasma and neutral atom number densities, respectively. These show that the two populations follow quite different plume expansion dynamics. The charge exchange plasma formed vertically above the thruster exit plane can be seen clearly in Fig. 4.

4.1 Ion Current Density

Angular profiles of ion current density are shown in Fig. 6 in which the Express data are compared with two different profiles measured for the SPT-100 in vacuum chambers by Manzella and Sankovic¹¹ and King.¹² There are several important points to be noted in this plot. First, while the laboratory data were obtained at 1 m from the thruster, as shown in Fig. 1, this is not the case for the Express measurements. To try to simplify the data comparisons, the Express data are scaled to values at 1 m from the thruster using a $1/r^2$ relation for the decay in ion current density with distance from the thruster. The accuracy of this relation will be considered later. The figure also indicates that there is considerable spread in the Express data. In some cases, for the same angular location, there is more than an order of magnitude variation. Reasons for some of these variations are discussed in Ref. 5 and include varying performance from different thrusters, and the possibility of partial obstruction of the sensor. Nevertheless, the data variations illustrate the challenge in obtaining good quality plume data under in-space conditions. Comparison of the three data sets in Fig. 6 shows the effect of the increased back-pressure found in vacuum chamber experiments. As the back pressure is decreased from the King experiment, to the Manzella experiment, to the Express flight, the ion current density profile shows a significant decay at high angles. Close to the plume axis, the Express data is consistently a factor of two to three lower than the laboratory data. It is not clear whether this difference is real or part of a systematic error in the Express measurements. As noted earlier, the development and assessment of Hall thruster plume models has been performed exclusively using laboratory data. The Express data is the only set of measurements of ion current density obtained in-space for the plume of a Hall thruster.

In Fig. 7, angular profiles of ion current density are shown in which the Express data is compared to three profiles obtained from the same simulation. The Express data and simulation profiles obtained at 1.40, 3.76, and 8.8 m from the thruster are each scaled using the $1/r^2$ relation to 1 m from the thruster. Comparison of the three simulation results indicates that the ion current density scales quite well with $1/r^2$. Near to the axis, the peak of the scaled ion current density decays with distance from the thruster, with a resulting slightly flatter distribution at larger angles. These differences are due primarily to collision effects. If there are no collisions in the plume, then the $1/r^2$ relation should hold for ion current density. However, the few collisions that do occur tend to scatter ions away from the axis leading to the relative reduction in ion current density there. The non-radial structure of the electric fields also changes the ion dynamics from the simple scaling law.

In Fig. 8, the same comparison is made for a simulation that employs the differential scattering cross sections from Ref. 2 for all atom-ion momentum exchange collisions, instead of isotropic scattering. The differences from the simulation profiles in Fig. 7 are small, and the scatter in the Express data makes it difficult to decide which modeling approach is preferred.

4.2 Primary Beam Ion Energy Distribution

The ion energy distribution measured on Express in the primary beam near to the centerline (at 7 deg.) and a distance of 3.76 m is now considered. In Fig. 8, the Express data is compared with the results of the simulation. Note, in terms of plotting style, that exact agreement between the data sets would mean that the solid line employed for the model results would go through the center of the horizontal bar of each column of the histogram used for the Express data. The RPA data measured in space provides a narrower distribution than profiles measured in ground facilities and this is perhaps explained by collisional broadening present in the vacuum tank experiments. In Fig. 8, there is clearly very good agreement between the simulation and the Express data.

4.3 Charge Exchange Ion Energy Distributions

The ion energy distribution obtained on Express at the large angle of 77 deg and a distance of 1.40 m (see Fig. 1) is now considered. This location is of particular interest since it is characterized primarily by charge exchange ions. Very few beam ions are expected to exit the Hall thruster at such large angles. In Fig. 9, the Express data are compared with the results from the simulation. Figure 9 includes a high energy structure measured on-board the Express spacecraft that extends up to values associated with primary beam ions of about 260 eV. These high energies are not simulated by the model, although the peak of the distribution at about 28 eV is very well predicted.

Finally, the ion energy distribution measured on SMART-1 at a distance of 0.55 m and an angle of 105 deg. is considered in Fig. 10. The SMART-1 distribution is similar to the large-angle distribution measured on Express. As shown in Fig. 10, the simulation again provides very good agreement with the data measured in-flight. A Langmuir probe located adjacent to the RPA on SMART-1 also provided measurements of several plasma properties at this same location. The measured values are compared to the corresponding simulation values in Table 2. With the exception of the electron temperature, which is significantly higher in the simulation, there is generally good agreement between the two sets of results. Also, note that the simulation explicitly assumes charge neutrality and so the ion and electron number densities are equal.

5. Concluding Remarks

A detailed hybrid particle-fluid PIC-DSMC model was applied to model the plume of an SPT-100 Hall thruster operating under the conditions experienced on the Russian Express and European SMART-1 spacecraft. Assessment of the model was performed through direct comparison of predictions of ion current density and ion energy distribution functions measured in space on these vehicles. These data represent the only measurements taken in the plume of a Hall thruster operated in space. Comparison of the simulation predictions with the data therefore allowed unique assessment of the plume model applied in the space environment.

In general, the comparisons indicated that the plume model was able to capture most of the features found in the measured data. In terms of the ion current density profile, it was found from the simulation that the simple scaling law of $1/r^2$ for ion current density applies quite well even when the plume expands far away from the thruster. Despite significant spread in the measured ion current density, agreement within a factor of two of most of the flight data was obtained at all angles for which data was measured. For the ion energy distribution measured in the primary ion beam, the simulation provided excellent agreement with the measured data. For the ion energy distributions measured in the charge exchange plasma on both Express and SMART-1, the simulation again provided good agreement. However, an extended high energy tail measured on Express was not simulated. Comparison of simulation results with various plasma properties measured by a Langmuir probe on SMART-1 also gave reasonable agreement.

In summary, this study has demonstrated that existing Hall thruster plume simulation codes are relatively successful in predicting the main features of the plasma plume based on the very limited sets of measured data obtained in space. Further improvement in the models requires additional in-space measurements most notably of ion current density in the charge exchange plasma. An important issue requiring further study is how best to determine the far-field boundary conditions required for the detailed fluid electron model.

6. Acknowledgments

Participation in the conference was made possible by funding from the 9th SCTC Organizing Committee. This work was funded by the Air Force Office of Scientific Research, grant FA9550-05-1-0042, with Dr. Mitat A. Birkan as the technical monitor. The author wishes to thank Martin Tajmar of ARCS for providing the SMART-1 data in electronic form.

7. References

- ¹ Boyd, I.D., "Review of Hall Thruster Plume Modeling," *Journal of Spacecraft and Rockets*, Vol. 38, 2001, pp. 381-387.
- ² Boyd, I. D. and Dressler, R. A., "Far Field Modeling of the Plume of a Hall Thruster," *Journal of Applied Physics*, Vol. 92, 2002, pp. 1764-1774.
- ³ Mikellides, I. G., Jongeward, G. A., Katz, I., and Manzella, D. H., "Plume Modeling of Stationary Plasma Thrusters and Interactions With the Express-A Spacecraft," *Journal of Spacecraft and Rockets*, Vol. 39, 2002, pp. 894-903.
- ⁴ Taccogna, F., Longo, S., and Capitelli, M., "Very-Near-Field Plume Simulation of a Stationary Plasma Thruster," *European Physical Journal: Applied Physics*, Vol. 28, 2004, pp. 113-122.
- ⁵ Manzella, D. H., Jankovsky, R., Elliott, F., Mikellides, I., Jongeward, G., and Allen, D., "Hall Thruster Plume Measurements On-Board the Russian Express Satellites," IEPC Paper 2001-044, October 2001.
- ⁶ Tajmar, M., Meissl, W., Gonzalez del Amo, J., Foing, B., Laakso, H., Noci, G., Capacci, M., Malkki, A., Schmidt, W., and Darnon, F., "Charge-Exchange Plasma Contamination on SMART-1: First Measurements and Model Verification," AIAA Paper 2004-3437, July 2004.

⁷ Bird, G. A., *Molecular Gas Dynamics and the Direct Simulation of Gas Flows*, Oxford University Press, Oxford, 1994.

⁸ Birdsall, C. K. and Langdon, A. B., *Plasma Physics Via Computer Simulation*, Adam Hilger Press, 1991.

⁹ Boyd, I. D. and Yim, J. T., "Modeling of the Near Field Plume of a Hall Thruster," *Journal of Applied Physics*, Vol. 95, 2004, pp. 4575–4584.

¹⁰ Mitchner, M. and Kruger, C.H., *Partially Ionized Gases*, Wiley Press, New York, 1973.

¹¹ Manzella, D. H. and Sankovic, J. M., "Hall Thruster Ion Beam Characterization," AIAA Paper 95-2927, July 1995.

¹² King, L. B., "Transport-Property and Mass Spectral Measurements in the Plasma Exhaust Plume of a Hall-Effect Space Propulsion System," Doctoral Thesis, Department of Aerospace Engineering, University of Michigan, 1998.

Table 1. Properties used in the simulation at the exit of the SPT-100 Hall thruster.

Inner Diameter (mm)	60
Outer Diameter (mm)	100
Plasma Density (m^{-3})	2.4×10^{17}
Neutral Density (m^{-3})	2.0×10^{18}
Ion Velocity (m/s)	18,455
Neutral Velocity (m/s)	280
Ion Temperature (eV)	1.0
Neutral Temperature (K)	750
Electron Temperature (eV)	6.0
Plasma Potential (V)	15

Table 2. Plasma properties at the location of the Langmuir probe used on SMART-1.

	SMART-1	Simulation
Ion Density (m^{-3})	$6-8 \times 10^{13}$	3.0×10^{13}
Electron Density (m^{-3})	$2.5-3.7 \times 10^{13}$	3.0×10^{13}
Electron Temperature (eV)	0.6-0.7	1.16
RPA Peak (V)	19	19

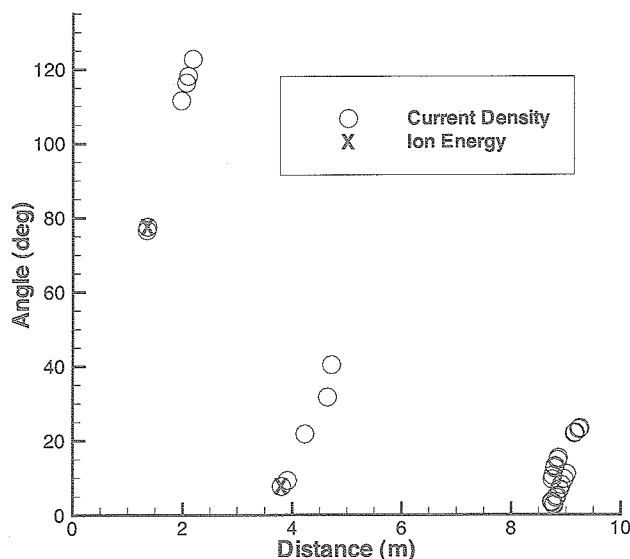


Fig. 1. Coordinates of the RPA sensors on Express.

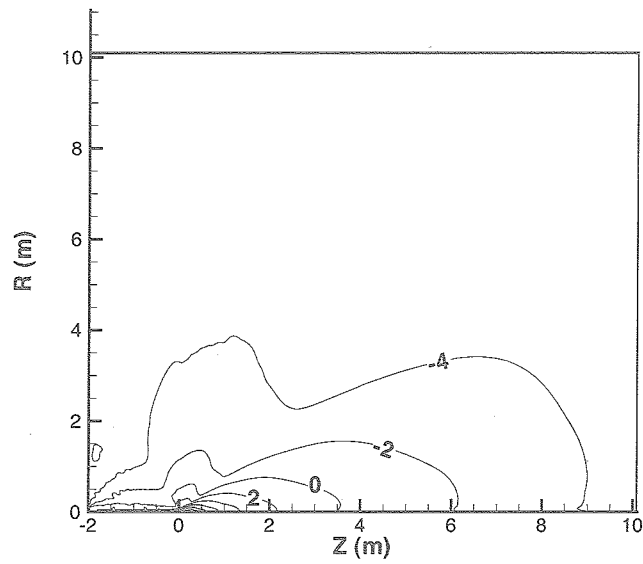


Fig. 2. Contours of plasma potential (V).

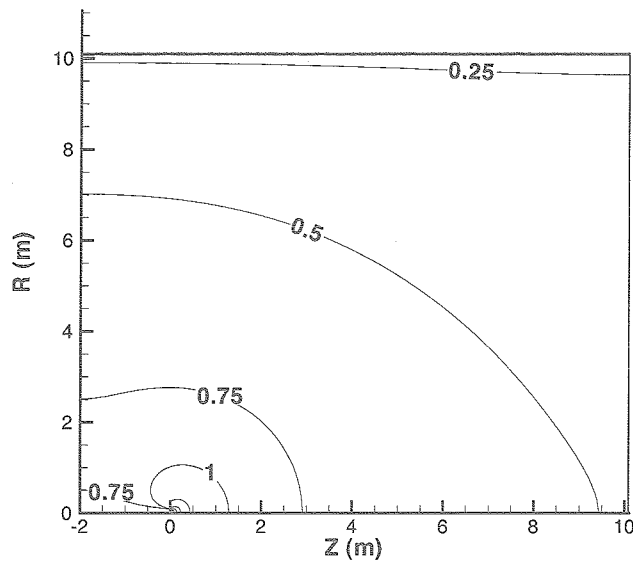


Fig. 3. Contours of electron temperature (eV).

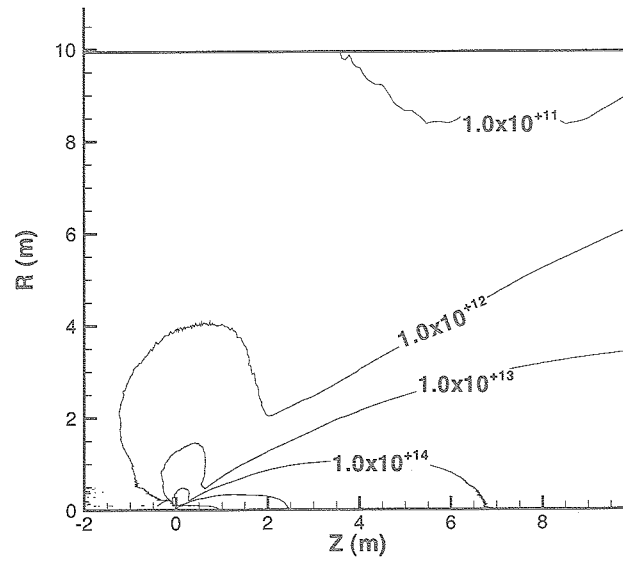


Fig. 4. Contours of plasma number density (m^{-3}).

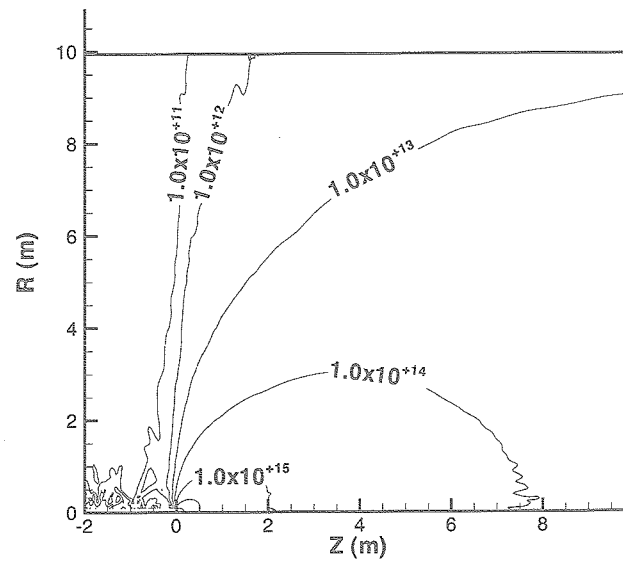


Fig. 5. Contours of atom number density (m^{-3}).

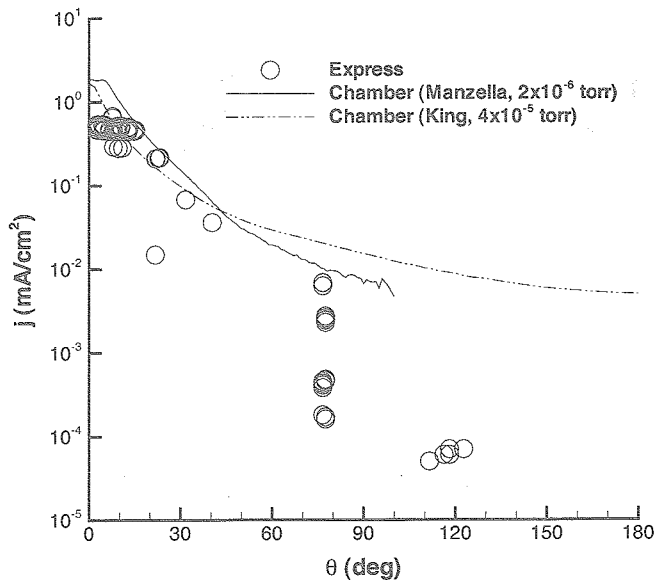


Fig. 6. Angular profiles of current density at 1 m from the thruster: comparison of Express and laboratory data.

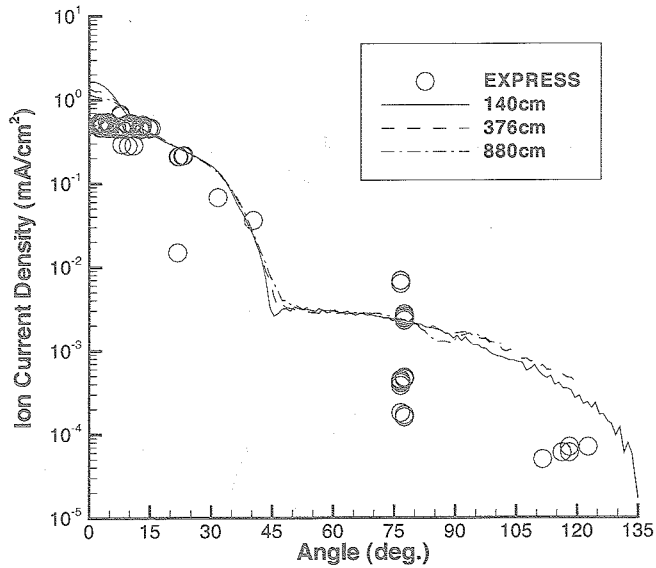


Fig. 7. Angular profiles of current density at 1 m from the thruster: comparison of Express and simulation data that employs isotropic scattering for atom-ion momentum exchange.

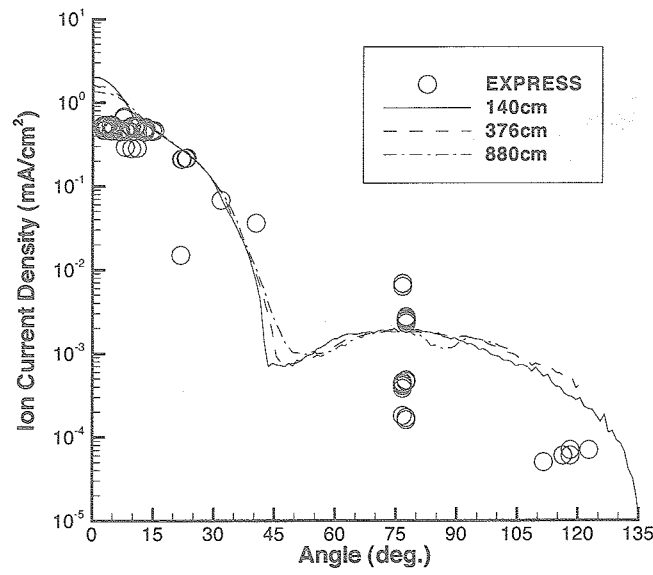


Fig. 8. Angular profiles of current density at 1 m from the thruster: comparison of Express and simulation data that employs differential scattering for atom-ion momentum exchange.

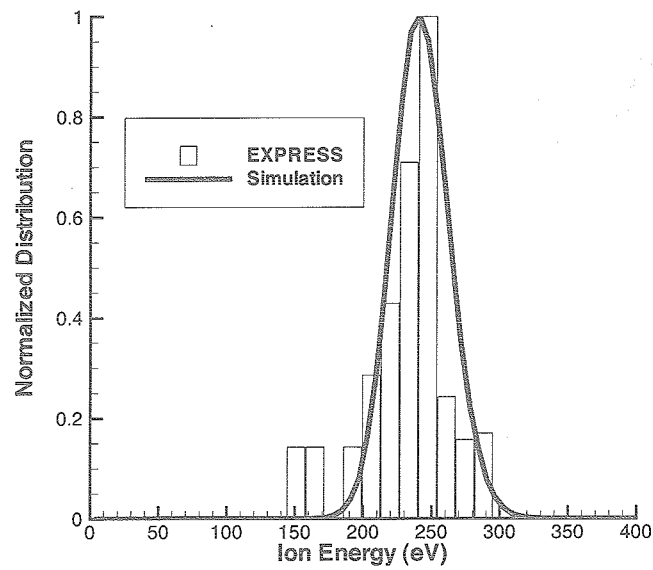


Fig. 9: Primary beam ion energy distribution function for Express ($z=3.76$ m, $\theta=7.5^\circ$).

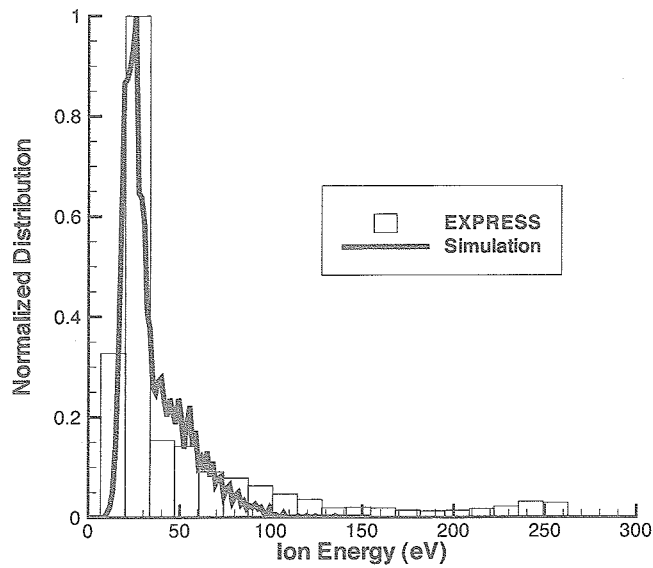


Fig. 10. Charge exchange ion energy distribution function for Express ($z=1.40$ m, $\theta=77.5^\circ$).

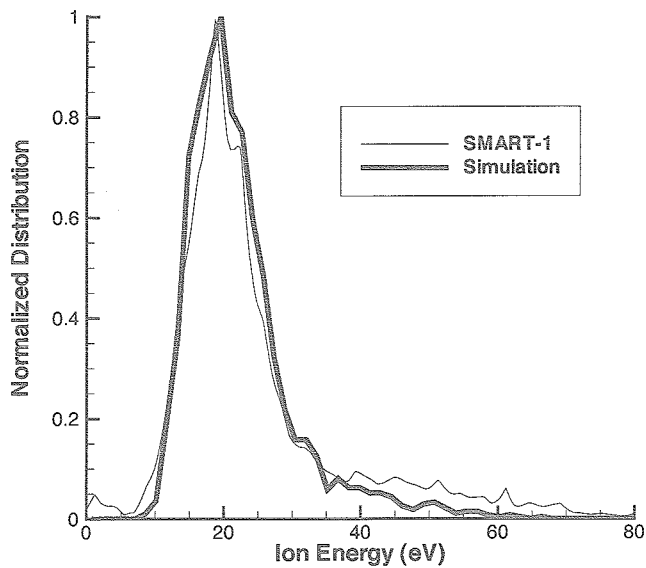


Fig. 11. Charge exchange ion energy distribution function for SMART-1 ($z=0.55$ m, $\theta=105^\circ$).